

# Washable Multilayer Triboelectric Air Filter for Efficient Particulate Matter PM<sub>2.5</sub> Removal

Yu Bai, Chang Bao Han, Chuan He, Guang Qin Gu, Jin Hui Nie, Jia Jia Shao, Tian Xiao Xiao, Chao Ran Deng, and Zhong Lin Wang\*

Efficient removal of particulate matter (PM) is the major goal for various air cleaning technologies due to its huge impact on human health. Here, a washable high-efficiency triboelectric air filter (TAF) that can be used multiple times is presented. The TAF consists of five layers of the polytetrafluoroethylene (PTFE) and nylon fabrics. Compared with traditional electrostatic precipitator, which requires a high-voltage power supply, the TAF can be charged by simply rubbing the PTFE and nylon fabrics against each other. The electrical properties of the TAF are evaluated through the periodic contacting–separating of the PTFE and nylon fabrics using a linear motor, and an open-circuit voltage of 190 V is achieved. After charging, the TAF has a removal efficiency of 84.7% for PM<sub>0.5</sub>, 96.0% for PM<sub>2.5</sub>, which are 3.22 and 1.39 times as large as the uncharged one. Most importantly, after washing several times, the removal efficiency of the TAF maintains almost the same, while the commercial face mask drops to 70% of its original efficiency. Furthermore, the removal efficiency of the PM<sub>2.5</sub> is very stable under high relative humidity. Therefore, the TAF is promising for fabricating a reusable and high-efficiency face mask.

of air pollutants, and the main constituent of the PMs is chemical mixtures, such as sulphate, nitrate, chloride, organic carbon, elemental carbon, iron, and calcium.<sup>[2]</sup> Generally, PMs are categorized according to the diameter of the particles, which ranges from several nanometers to tens of micrometers. Take PM<sub>2.5</sub>, for example, which defined as particulate matter with an aerodynamic diameter less than 2.5 μm, they could penetrate human bronchi and lungs leading to respiratory and cardiovascular disease even cancer.<sup>[3]</sup> Some researches also show the relation between the long-term exposure to PM<sub>2.5</sub> and the increase of the morbidity and mortality.<sup>[4]</sup> In Beijing, 42 d of a year were heavily PM<sub>2.5</sub> polluted (air quality is considered “heavily polluted” if 24 h average concentrations of PM<sub>2.5</sub> are 150–250 μg m<sup>-3</sup>) in 2015.<sup>[5]</sup> Various materials and technologies have been developed for air filtration, such as

## 1. Introduction

Air pollution has raised serious concern recently due to its hazardous threat to public safety and health. Anthropogenic activities, such as automobile exhaust, burn farming, construction, and burning of coal, have resulted in severe air pollution in many developing countries.<sup>[1]</sup> Particulate matter (PM) pollution has become one of the most serious issues among various types

electrostatic precipitator, electrospinning, metal-organic framework (MOF)-based membranes, and melt-blown polymers.<sup>[6]</sup> However, there are some drawbacks in these technologies: for electrostatic precipitator, the high voltage requires a huge consumption of energy and also leads to the production of ozone, which is harmful to human health;<sup>[7]</sup> while for the electrospinning polymers, the mechanical strength of the materials still needs to be enhanced in the future and the filter element needs to be replaced frequently to maintain the high removal efficiency.<sup>[8]</sup> Therefore, it is necessary to find a low-cost, long-service life, and low-energy consumption way to realize the effective filtration of the PMs.

Invented in 2012, triboelectric nanogenerator (TENG) is capable of converting low-frequency mechanical energies into electricity or sensing mechanical agitations.<sup>[9]</sup> Based on the coupling between the triboelectric effect and electrostatic induction, TENG has proven to be a cost-effective and environmentally friendly technology for mechanical energy harvesting and self-powered devices and systems.<sup>[10]</sup> One typical characteristic of the TENG is its high open-circuit voltage, which can be reached up to several hundred volts,<sup>[11]</sup> hence making it a strong candidate for air purification. Utilizing the rotating TENG as a power supply, Chen et al. first introduced a self-powered air cleaning system for removing SO<sub>2</sub> and PMs in 2014;<sup>[12]</sup> and Gu et al. developed a rotating TENG enhanced polyimide nanofiber filter for efficient PM removal.<sup>[13]</sup> Furthermore, based on a vibration TENG, which make use of the natural vibration

Y. Bai, Dr. C. B. Han, Dr. C. He, G. Q. Gu, J. H. Nie, J. J. Shao, T. X. Xiao, C. R. Deng, Prof. Z. L. Wang  
CAS Center for Excellence in Nanoscience  
Beijing Key Laboratory of Micro-nano Energy and Sensor  
Beijing Institute of Nanoenergy and Nanosystems  
Chinese Academy of Sciences  
Beijing 100083, China  
E-mail: zlwang@gatech.edu

Y. Bai, G. Q. Gu, J. H. Nie, J. J. Shao, T. X. Xiao, C. R. Deng  
School of Nanoscience and Technology  
University of Chinese Academy of Sciences  
Beijing 100049, China  
Prof. Z. L. Wang  
School of Materials Science and Engineering  
Georgia Institute of Technology  
Atlanta, GA 30332-0245, USA

 The ORCID identification number(s) for the author(s) of this article can be found under <https://doi.org/10.1002/adfm.201706680>.

DOI: 10.1002/adfm.201706680

of the car's tailpipe, Han et al. fabricated a self-powered triboelectric filter that effectively captures the PMs from automobile exhaust fumes.<sup>[14]</sup>

In this study, we present a washable multilayer triboelectric air filter (TAF) for efficiently removing the PMs. The TAF consists of multipieces of nylon fabrics and polytetrafluoroethylene (PTFE) fabrics, which can be charged through contact electrification. Compared with the TAF before charging, the removal efficiency of the charged TAF can be greatly enhanced due to electrostatic attraction. After charging, the removal efficiency of PM<sub>0.5</sub> and PM<sub>2.5</sub> are increased from 26.3% to 84.7% and 69.1% to 96.0%, respectively. Another advantage of the TAF is that it can be easily cleaned with commercial detergent and the removal efficiency was barely changed, while the

commercial face mask drops to 70% of its original efficiency. Furthermore, the removal efficiency of the PM<sub>2.5</sub> maintained at a high level (>91.8%) in a long-term test of 12 h and under high relative humidity, the removal efficiency of PM<sub>2.5</sub> is also stable throughout the whole measurement.

## 2. Results and Discussions

Figure 1a shows the schematic illustration of the measurement setup for determining the flow rate, pressure drop and PM removal efficiency of TAF. The TAF is fixed at the junction of two acrylic tubes; the pressure drop and flow rate are measured by a pressure gauge and a flow meter, respectively.

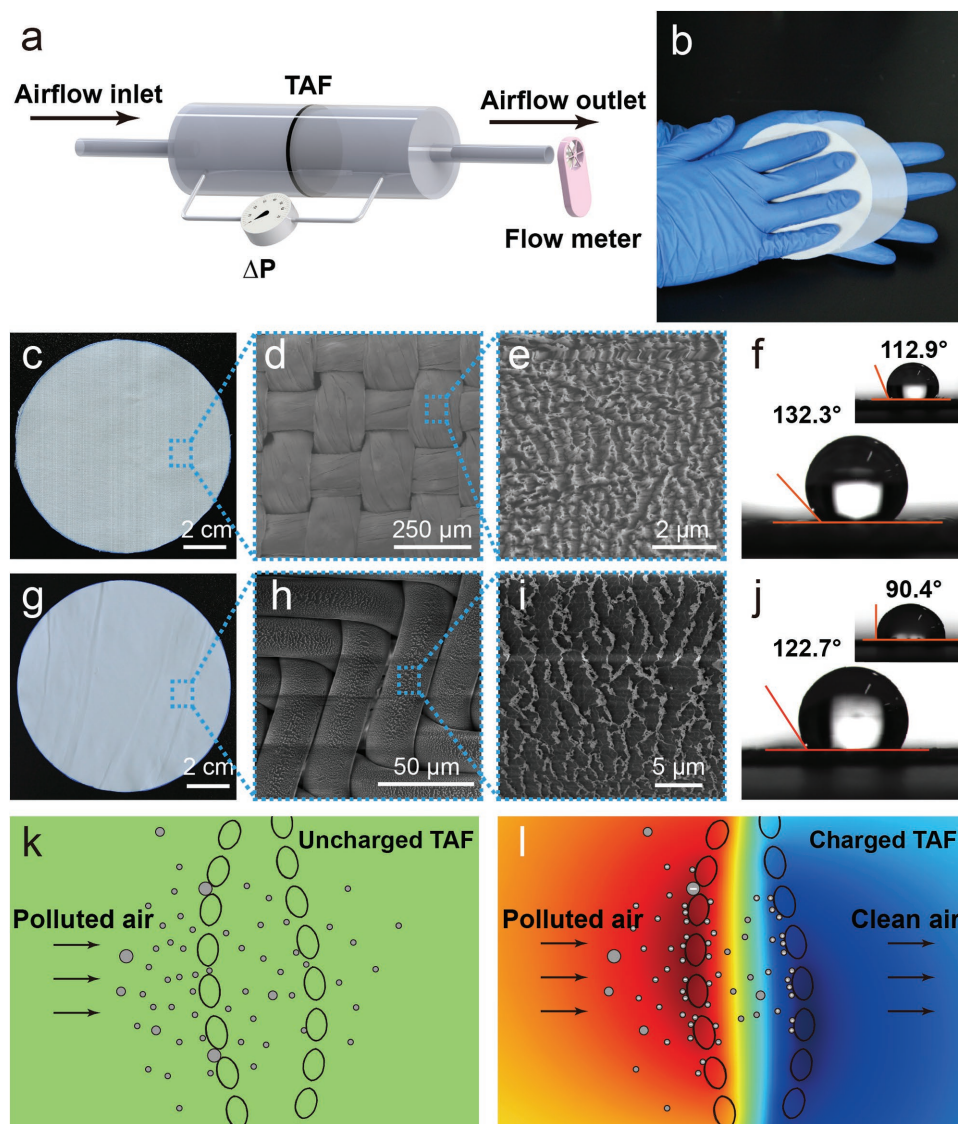


**Figure 1.** a) Schematic illustration of the setup for the measurement of the flow rate, pressure drop, and PM removal efficiency. b) Photoimage of the rubbing process for charging the TAF. c) The optical image, d) magnified scanning electron microscope (SEM) image of the surface, and e) SEM image of the etched nanostructures of the PTFE fabric. f) The profile of a water drop on an ICP-etched PTFE fabric. The inset shows a water drop on the unetched PTFE fabric. g) The optical image, h) SEM image of the surface, and i) SEM image of the etched nanostructures of the nylon fabric. j) The profile of a water drop on an ICP-etched nylon fabric. The inset shows a water drop on the unetched nylon fabric. k, l) Schematic illustration of the filtration mechanism of the k) uncharged TAF and the l) charged TAF.

By simply rubbing the PTFE and nylon fabrics against each other for about 2 min by hands as shown in Figure 1b, a high electric field is formed between nylon fabric and PTFE fabric through contact electrification. The reasons for selecting PTFE and nylon are twofold: first, they are at the opposite end of the triboelectric series, indicating their large difference in ability to attain electrons;<sup>[15]</sup> second, PTFE is a typical electret and the negative charges could maintain on the surface for a long time,<sup>[16]</sup> and nylon has a dipole moment of 3.67, generally, polymers with higher dipole moment could remove the PMs efficiently and a high removal efficiency is achieved by the strong adhesion between nylon fibers and PMs.<sup>[6c]</sup> Figure 1c shows the optical image of the PTFE fabric and the magnified scanning electron microscope (SEM) image of the surface is shown in Figure 1d. In order to increase the triboelectric charge density on the surface and thus improve the removal efficiency, nanostructures are created on the surface of the PTFE fabric by inductively coupled plasma (ICP).<sup>[17]</sup> The SEM image of the nanostructures is shown in Figure 1e. The ICP-etched surface of the PTFE fabric has a contact angle of 132.3° for water drop compared to the original ones (112.9°), as shown in Figure 1f, indicating the PTFE fabric with nanostructure is more hydrophobic and might be used in high humid environment. The optical image and the magnified SEM image of nylon fabric are shown in Figure 1g and Figure 1h, respectively. The nylon fabric is also etched by ICP (Figure 1i) and the contact angle increased about 30° (Figure 1j, 90.4°–122.7°).

Figure 1k,l illustrates the working mechanism of the TAF. As shown in Figure 1k, for the uncharged filter, the PMs are mainly removed by mechanical filtration, such as interception, inertial impaction, Brownian diffusion, and gravitational

settling. For particles larger than 0.3  $\mu\text{m}$ , interception and inertial impaction are the main capture mechanisms. Brownian diffusion plays a vital role for the particles with size below 0.1  $\mu\text{m}$  and it becomes more significant with decreased particle size.<sup>[18]</sup> Gravitational settling can be ignored for the particles smaller than 0.5  $\mu\text{m}$  because it is so small compared with other forces. In polluted air, the sub-micrometer particles have a greater damage to human health because they are able to penetrate into the bloodstream and translocate to other parts of the body.<sup>[19]</sup> However, the effect of mechanical filtration for these particles is limited. Through sufficient rubbing between nylon and PTFE fabrics, nylon is positively charged and PTFE is negatively charged according to the triboelectric series.<sup>[15]</sup> Thus, an electric field is built between nylon and PTFE, as shown in Figure 1l. In general, the fibers are more effective in collecting PMs with the diameter larger than the spacing of the fibers. With the formed electric field, the particle with a smaller size can be effectively removed through electrostatic attraction.

The effective formation of the electric fields on the surfaces of nylon and PTFE fabrics is evaluated in the contact-separation mode of TENG, as illustrated in Figure 2a. The PTFE and nylon fabrics with the size of 5 cm  $\times$  5 cm are placed on the supporting acrylic substrate and then mounted on a linear motor that brought the fabrics in contact periodically. On the back sides of the PTFE and nylon fabrics are aluminum (Al) electrodes. The periodic contacting-separating of the fabrics produces an alternating current in the external circuit, and the underlying mechanism has been described elsewhere.<sup>[20]</sup> Figure 2b–d shows the open-circuit voltage ( $V_{OC}$ ), the short-circuit current ( $I_{SC}$ ),

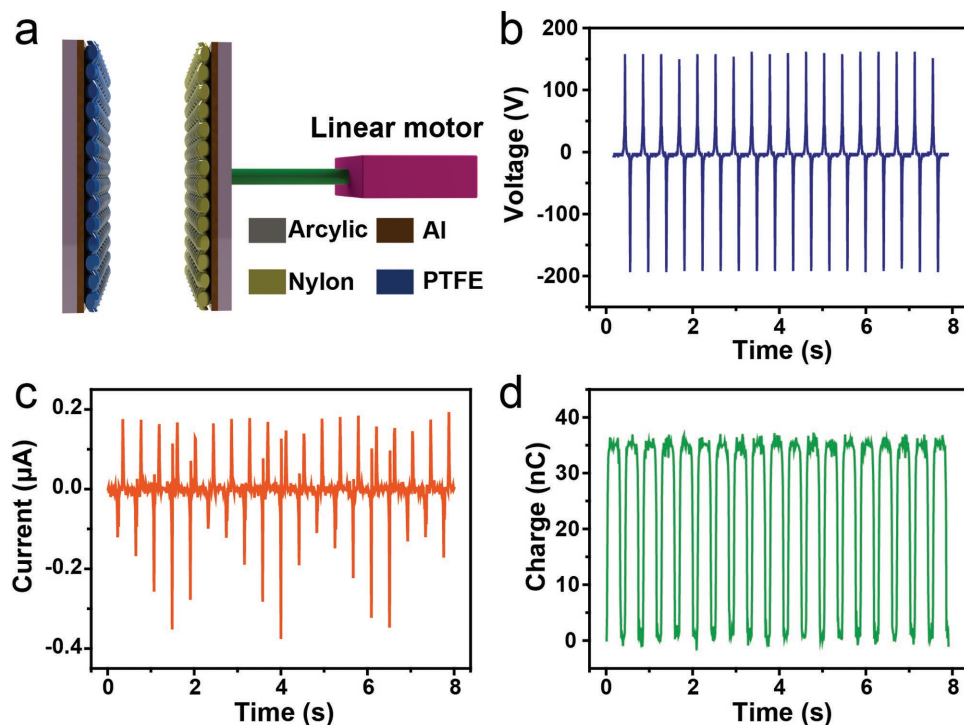


**Figure 2.** a) Schematic illustration of the PTFE fabric and nylon fabric as contact layers in contact-separation mode. b) The open-circuit voltage. c) The short-circuit current. d) The transferred charges.

and the transferred charge ( $\Delta Q$ ) of the TENG at a frequency of 2.4 Hz. The maximum  $V_{OC}$  is about 190 V, the peak value of  $I_{SC}$  could reach 0.35  $\mu A$ , and the amount of transferred charge  $\Delta Q$  is about 35 nC. When the distance between PTFE fabric and nylon fabric is less than 0.1 mm, the space electric field can reach up to  $\approx MV m^{-1}$ , (Movie S1, Supporting Information) which is sufficient for removing particles by electrostatic interactions.

The removal efficiency of the uncharged and charged TAF is thoroughly studied in a 30  $m^3$  lab, where the PMs are generated by burning cigarettes. The diameter of the generated smoke distributes from  $<0.3 \mu m$  to  $>10 \mu m$ , and most of the particulate matter is  $<1 \mu m$ .<sup>[21]</sup> The concentration of  $PM_{2.5}$  at the entrance of the setup was greater than or equivalent to 300  $\mu g m^{-3}$ . To make sure the PTFE and nylon fabrics were uncharged, the PTFE and nylon fabrics were soaked in the

water for 10 min and then dried slowly in atmosphere. The concentrations of the particles at the inlet and outlet were measured by a handheld particle counter, and the removal efficiency  $\eta$  can be calculated from the following equation

$$\eta = \frac{C_{in} - C_o}{C_{in}} \times 100\% \quad (1)$$

where  $C_o$  and  $C_{in}$  represent the cumulative mass concentration ( $\mu g m^{-3}$ ) of particles at the outlet and inlet, respectively. **Figure 3a** compares the PM removal efficiency of the uncharged and charged filters for the PMs with different sizes. The flow rate is 6  $L min^{-1}$  (unless otherwise specified, the flow rate is always 6  $L min^{-1}$  in this paper). We can see that for the uncharged TAF, the removal efficiencies increase as the particle size increases, which is in accordance with our previous

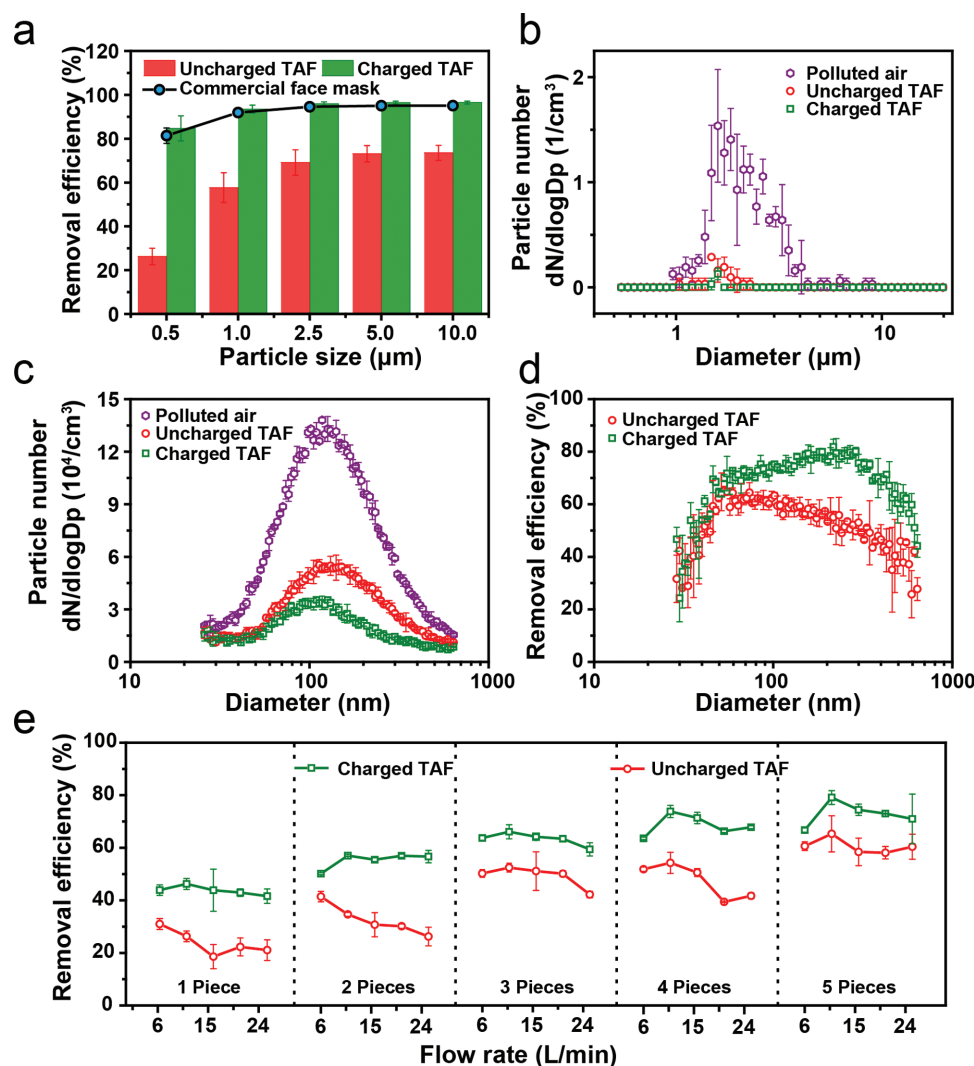


**Figure 3.** a) The removal efficiency of the uncharged and charged TAF with five pieces of PTFE and nylon fabrics. b) Particle size distribution of the PMs in the polluted air, air that filtered by the uncharged TAF, and air that filtered by the charged TAF in the range of 0.542–19.81  $\mu m$ . c) Particle size distribution of the PMs in the polluted air, air that filtered by the uncharged TAF, and air that filtered by the charged TAF in the range of 25.9–637.8 nm. d) Comparison of the removal efficiency of the uncharged and charged TAF in the diameter region of 25.9–637.8 nm. e) The removal efficiency of the uncharged and charged TAF (1–5 pieces) for the PMs with a diameter of 131 nm under different flow rates ranging from 6 to 25.2  $L min^{-1}$ .

analysis. After sufficient charging between the fabrics through rubbing, the removal efficiency of the TAF for all the PMs is greatly enhanced, where the removal efficiencies for the PM<sub>0.5</sub>, PM<sub>1.0</sub>, PM<sub>2.5</sub>, PM<sub>5.0</sub>, and PM<sub>10.0</sub> are increased from 26.3%, 57.7%, 69.1%, 73.2%, and 73.5% to 84.7%, 93.5%, 96.0%, 96.5%, and 96.5%, respectively. It is clear that the smaller particle sizes, the greater enhancement in removal efficiency. For PM<sub>0.5</sub>, the removal efficiency of the charged TAF is 3.22 times as large as that of the uncharged TAF. Furthermore, the charged TAF is also compared with the commercial face mask in Figure 3a. It can be seen that the removal efficiency of the TAF is comparable to that of the commercial face mask.

To gain a better understanding of the capability of the TAF for removing particles of different sizes, the distribution of particles in polluted air, air that filtered by the uncharged TAF, and air that filtered by the charged TAF are presented and compared in Figure 3b,c under the flow rate of 15.6 L min<sup>-1</sup>. In Figure 3b, the particles of the size in the range of 0.542–19.81 μm are measured by an aerodynamic particle sizer (3321, TSI, USA). It can be seen that the number of the particles are on the order of 1 cm<sup>-3</sup>. Both the uncharged and charged TAF have high removal efficiency over 80%, indicating the mechanical filtration is dominant in the filtration process. In Figure 3c, the distribution of the particles in the range of 25.9–637.8 nm, which is measured by a scanning mobility particle sizer (SMPS 3938L75, TSI, USA). Clearly, the number of the particles in the nm range, which is on the order of 10<sup>4</sup> cm<sup>-3</sup>, is significantly higher than the particles in the μm range. In addition, we can see that in the polluted air, the number of the particles peaks around 117.6 nm, and has a value of 138 000 cm<sup>3</sup>. After filtration, the number

of the particles in the measured range is both decreased notably, especially for the charged TAF. The corresponding removal efficiency of the uncharged TAF and charged TAF is illustrated in Figure 3d. For the particles ranging from 216.7 to 572.5 nm, the removal efficiency of the charged TAF is improved by over 50% than the uncharged TAF. The result demonstrates that in addition to the mechanical filtration, the electrostatic attraction also plays an important role in removing the particles in the nm range, hence further increase the removal efficiency. Moreover, the removal efficiency of the TAF with different pieces (from 1 to 5 pieces) for the particles with the diameter of 131 nm is obtained at a different flow rate (from 6 to 25.2 L min<sup>-1</sup>), as shown in Figure 3e. It is straightforward that the removal efficiency is higher when the TAF consists of more pieces of PTFE fabrics and nylon fabrics and the charged TAF has higher removal efficiency than the uncharged one. What is more, the main trend of removal efficiency for uncharged TAF is slowly decays with the increase of the flow rate, while it keeps almost stable for charged TAF. This might be attributed to the different filtration mechanism: for the uncharged TAF, the particles mainly filtered by interception, inertial impaction, Brownian diffusion, and gravitational settling, and the particles with high speed are difficult to be deposited on the filter. As to the charged TAF, the electric field force is stronger than the force of Brownian diffusion or gravity. The increased flow rate also results in the slight vibration between the nylon and PTFE fabrics forming high triboelectric field, and thus leading to an enhanced contact electrification and electrostatic attraction, which makes the removal efficiency keeps stable.

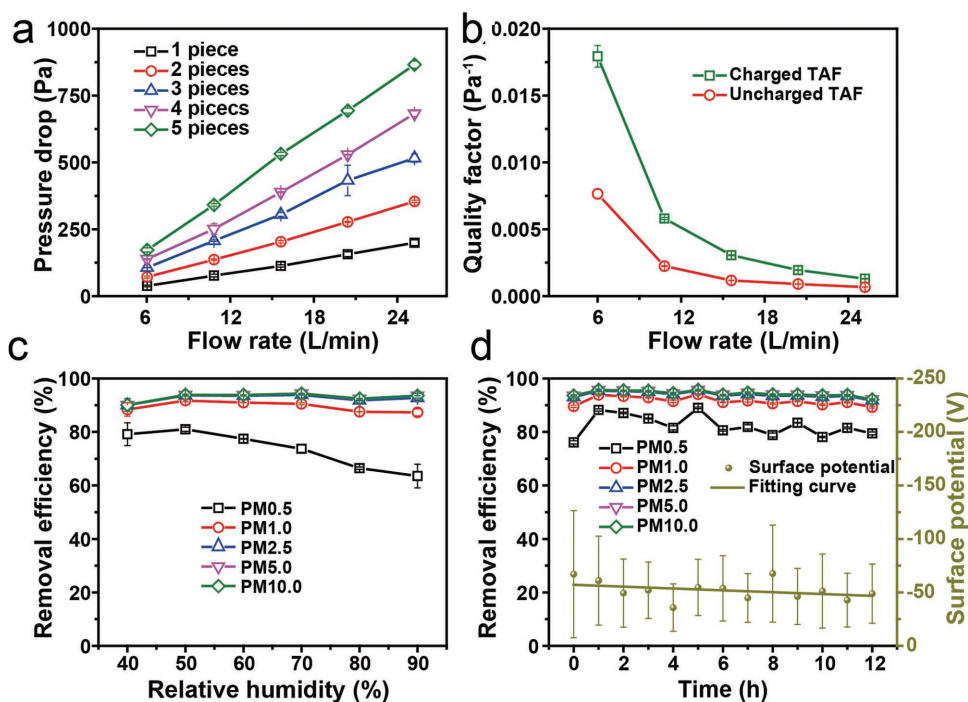


**Figure 4.** a) Pressure drop of the air filter with different pieces. b) Quality factor of the uncharged and charged TAF with 5 pieces under the flow rate of 6–25.2 L min<sup>-1</sup>. c) The removal efficiency of the TAF for PM<sub>2.5</sub>–PM<sub>10.0</sub> under various relative humidity. d) 12 h test of the removal efficiency of the TAF and the surface potential of the PTFE fabric.

Another important index to evaluate the overall filtration capacity of the air filters is the quality factor (QF), which is defined by the following formula

$$QF = \frac{-\ln(1-\eta)}{\Delta p} \quad (2)$$

where  $\eta$  represents the removal efficiency and  $\Delta p$  represents the pressure drop. Figure 4a shows the pressure drop of the charged TAF at a different flow rate. We can see that for the TAF with different pieces, the pressure drop is proportional to the flow rate. This is in good agreement with the Darcy's theory and is consistent with other studies.<sup>[6d,22]</sup> The QF of the

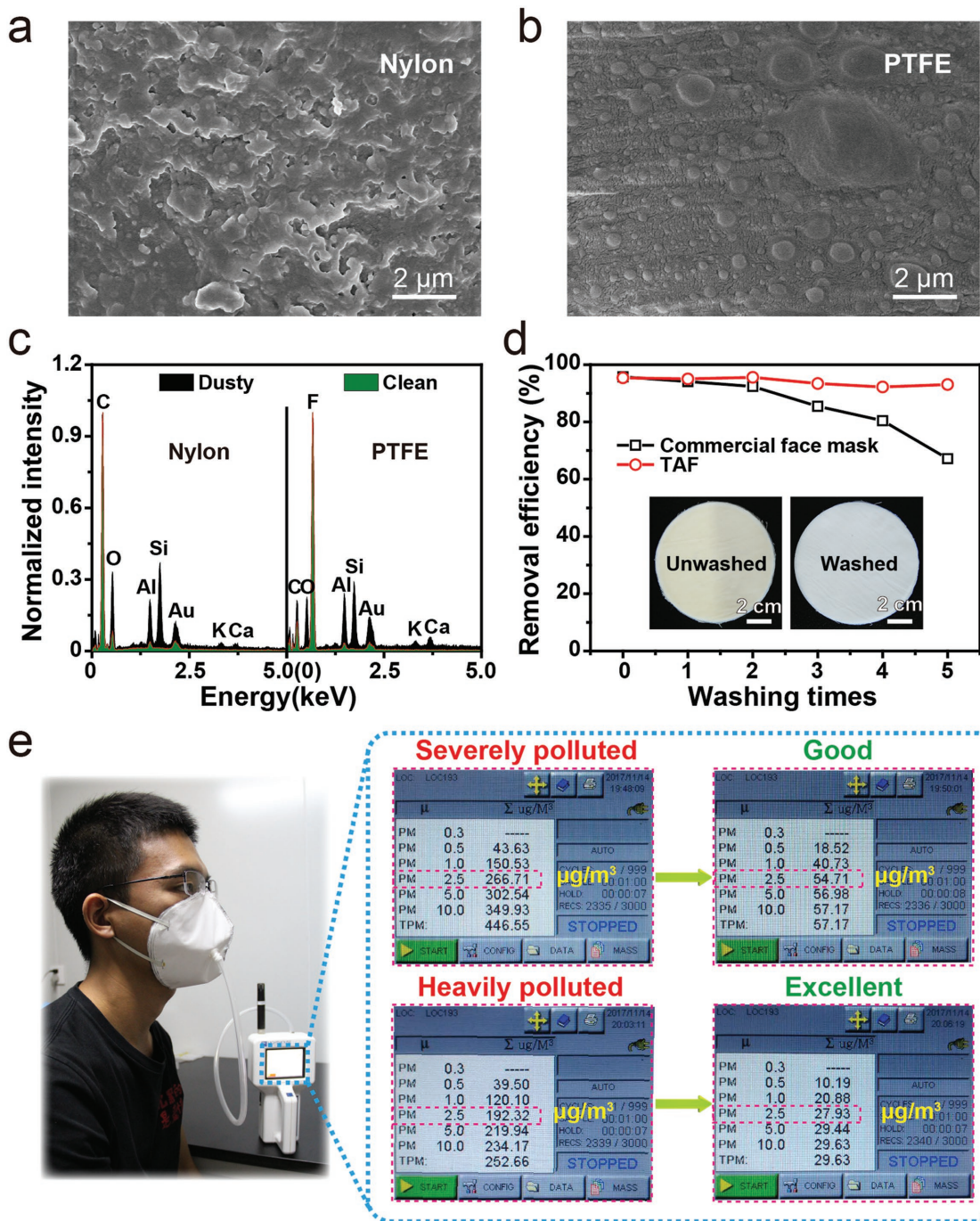


**Figure 5.** a) SEM image of nylon fabric after the filtration. b) SEM image of PTFE fabric after the filtration. c) The EDS spectra of the nylon and PTFE fabric before and after the filtration. d) The removal efficiency of as-fabricated TAF and a commercial face mask washed for 0–5 times. The insets are photo images of the unwashed and washed TAF. e) The schematic diagram of the measurement of the removal efficiency of the face mask made of the TAF. The face mask was worn by a man for 4 h. The concentration of PM<sub>2.5</sub> changed from severely polluted to good, and from heavily polluted to excellent.

uncharged and charged TAF under different flow rates is shown in Figure 4b. At a flow rate of  $6 \text{ L min}^{-1}$ , the  $QF$  of the charged filter increased by 1.3 times than the uncharged filter. Besides, as shown in Figure 4c, for different humid conditions (40–90%), the removal efficiency of the charged TAF for  $\text{PM}_{1.0}$ – $\text{PM}_{10.0}$  maintains above 87%, while the removal efficiency for  $\text{PM}_{0.5}$  declines to 63.5% (still larger than the uncharged TAF). Besides, the removal efficiency for  $\text{PM}_{2.5}$  is also retained at a high level in condition of 60% humidity for 2 h (Figure S1, Supporting Information). The high removal efficiency in high humid conditions can be attributed to the nanostructures on the surface of the PTFE and nylon fabrics, which enhance the hydrophobicity and reduce the moisture to the triboelectric effect. Furthermore, a 12 h measurement was taken to test the removal efficiency of the charged TAF over time. As shown in Figure 4d, the high removal efficiency over 89% for  $\text{PM}_{1.0}$ – $\text{PM}_{10.0}$  is obtained for the whole measurement time. As for  $\text{PM}_{0.5}$ , the charged TAF has a relatively low removal efficiency, but still larger than 76%. Besides, the surface potential of the PTFE fabric is also presented in Figure 4d. It can be seen that the surface potential slightly decreases over the measurement time, which ensures the high removal efficiency of the charged TAF.

After continuous filtration of the PMs for 5 h, the SEM images of the nylon fabric and PTFE fabric are presented in Figure 5a,b. Clearly, after the filtration, the surfaces are covered by the PMs, where the nanostructures are barely seen. An energy-dispersive spectroscopy (EDS) of the TAF after the filtration is shown in Figure S2 (Supporting Information) to investigate the chemical composition of the collected PMs. No additional chemical element is observed in the EDS spectra, which means the constituents of the PMs of the smoke of a cigarette are consistent with the TAF's chemical composition. This is in good agreement with other studies.<sup>[23]</sup> To further testify the PMs are absorbed by the TAF, a solid aerosol generator (TOPAS SAG 410/L, Germany) was used to generate PMs. Figure 5c shows the EDS spectra of the filtrated TAF. Some elements, such as O, Al, and Au increase notably, and other elements such as Si, K, and Ca are found, which indicates that the PMs are effectively removed by the TAF. After the long-term test, the color of the filter changed from white to yellow (inset of Figure 5d). Additionally, the PTFE fabric and nylon fabric can be simply cleaned with water and detergent. Figure 5d shows the removal efficiency of the charged TAF and a commercial face mask after being washed for several times. The removal efficiency of the TAF still maintains at a high level over 92% after being washed up for 5 times, while the removal efficiency of the commercial face mask declines to about 67%. This proves that the TAF is washable and still maintains high removal efficiency.

The TAF consisting of PTFE fabric and nylon fabric is simple, washable, and high-efficient in removing the PMs. Figure 5e illustrates a face mask made of the TAF to verify the filter's performance under actual usage condition. A rubber tube is connected to the face mask and the particle counter to get the real-time data of the concentration of the PMs filtered by the face mask in the  $30 \text{ m}^3$  lab. According to the conversion relationship between air quality index and  $\text{PM}_{2.5}$ ,<sup>[5]</sup> air quality is considered "severely polluted" and "heavily polluted" if 24 h average concentrations of  $\text{PM}_{2.5}$  are  $>250 \text{ } \mu\text{g m}^{-3}$  and  $150\text{--}250 \text{ } \mu\text{g m}^{-3}$ , respectively. After the face mask was worn by a

man for 4 h in daily life, for severely polluted condition, where the concentration of  $\text{PM}_{2.5}$  is  $266.71 \text{ } \mu\text{g m}^{-3}$ , the  $\text{PM}_{2.5}$  in the face mask decreased to  $54.71 \text{ } \mu\text{g m}^{-3}$ . As for heavily polluted condition, where the concentration of  $\text{PM}_{2.5}$  is  $192.32 \text{ } \mu\text{g m}^{-3}$ , the  $\text{PM}_{2.5}$  in the face mask can be decreased to  $27.93 \text{ } \mu\text{g m}^{-3}$ . The measurements prove that the TAF is efficient in real-life applications and can be a strong candidate in fabricating face masks.

### 3. Conclusion

In summary, we demonstrate an efficient triboelectric air filter consisting of PTFE fabrics and nylon fabrics. By rubbing the PTFE and nylon fabrics against each other, a high-voltage electric field is generated on the surface of the fabrics, hence introducing the electrostatic attraction in removing the PMs. An open-circuit voltage of 190 V is achieved by the periodic contacting-separating of the PTFE and nylon fabrics using a linear motor. After sufficient charging between the fabrics, the removal efficiency of the TAF for the  $\text{PM}_{0.5}$  and  $\text{PM}_{2.5}$  is increased from 26.3% to 84.7% (222.2% increased) and 69.1% to 96.0% (38.8% increased). Furthermore, in both a 12 h durability test and in a high humid test, the high removal efficiency is also maintained. And the removal efficiency barely changed after five washing cycles. Therefore, the TAF is high-efficiency and washable in real-life applications and is promising to fabricate as face masks in the future.

### 4. Experimental Section

**Fabrication of TENG and Electrical Measurement:** To fabricate the TENG, two pieces of acrylic were shaped by a laser cutter (PLS6.75, Universal Laser Systems, USA) as substrates with dimensions of  $5 \text{ cm} \times 5 \text{ cm} \times 0.4 \text{ cm}$ . Two layers of  $50 \text{ } \mu\text{m}$  aluminum foil adhered to the substrate in a size of  $5 \text{ cm} \times 5 \text{ cm}$  as the electrode. PTFE fabric and nylon fabric in a size of  $5 \text{ cm} \times 5 \text{ cm}$  were assembled on the aluminum electrode, respectively. Finally, lead wires were utilized to connect the two electrodes for electrical measurement. The short-circuit current and transferred charges were measured by an electrometer (Keithley 6514, Tektronix Company, USA). The open-circuit voltage was measured by a digital oscilloscope (Agilent DSO-X 2014A, Agilent Technologies, USA). The surface potential of the PTFE fabric was measured by an electrostatic voltmeter (Model 344, Trek Company, USA).

**Fabrication of the Nanostructure:** The PTFE fabric and nylon fabric were first washed with menthol, isopropyl alcohol, and deionized water, consecutively, and then blown dry with nitrogen. Subsequently, a thin film of Cu with a thickness of 5 nm was sputtered onto the PTFE and nylon surfaces as the mask for the etching process. Then the ICP reactive ion etching was used to produce the aligned nanowires on the surface. Specifically, Ar,  $\text{O}_2$ , and  $\text{CF}_4$  gases were introduced in the ICP chamber with the flow ratio of 15.0, 10.0, and 30.0 sccm, respectively. One power source of 400 W was used to generate a large density of plasma and the other power of 100 W was used to accelerate the plasma ions. The PTFE film was etched for 40 s to get the nanostructure.

**PM Generation and Efficiency Measurement:** The PM generation and efficiency measurement were tested in a  $30 \text{ m}^3$  lab. The PM used in this work was generated by burning a cigarette and a solid aerosol generator (TOPAS SAG 410/L, Germany). By diluting the smoke PM by air and waiting for 15 min to make smoke evenly dispersed in the air, the inflow concentration was controlled to a hazardous pollution level equivalent to the  $\text{PM}_{2.5}$  index of  $\geq 300$ . A handheld particle counter (Hand-held 3016-IAQ, Lighthouse, USA), a scanning mobility particle sizer (SMPS 3938L75, TSI, USA), and an aerodynamic particle sizer (3321, TSI, USA)

were used to detect the PM particle number concentration before and after filtration. The removal efficiency was calculated by comparing the number concentration before and after filtration.

**Pressure Drop Measurement:** The pressure drop was measured by a differential pressure gauge (Testo 510, Germany) and the flow rate was measured by a flowmeter (Testo 450-V1, Germany).

**Characterization:** The SEM images were taken by a SEM (SU8020, Hitachi Company, Japan) with an acceleration voltage of 5 kV for imaging.

## Supporting Information

Supporting Information is available from the Wiley Online Library or from the author.

## Acknowledgements

Y.B. and C.B.H. contributed equally to this work. This research was supported by the “Thousands Talents” program for the pioneer researcher and his innovation team, the National Key R & D Project from Minister of Science and Technology (Grant No. 2016YFA0202704), National Natural Science Foundation of China (Grant No. 51432005, 51608039, 5151101243, and 51561145021), Natural Science Foundation of Beijing, China (Grant No. 4154090), and Beijing Municipal Science & Technology Commission (Grant No. Z171100000317001).

## Conflict of Interest

The authors declare no conflict of interest.

## Keywords

nylon fabrics, PM<sub>2.5</sub>, polytetrafluoroethylene (PTFE) fabrics, triboelectric air filters, washable filters

Received: November 16, 2017

Revised: December 21, 2017

Published online:

- [1] a) F. Laden, L. M. Neas, D. W. Dockery, J. Schwartz, *Environ. Health Perspect.* **2000**, *108*, 941; b) Y. L. Sun, G. S. Zhuang, W. Ying, L. H. Han, J. H. Guo, D. Mo, W. J. Zhang, Z. F. Wang, Z. P. Hao, *Atmos. Environ.* **2004**, *38*, 5991.
- [2] a) R. M. Harrison, A. M. Jones, R. G. Lawrence, *Atmos. Environ.* **2004**, *38*, 4531; b) J. H. Seinfeld, *Science* **1989**, *243*, 745.
- [3] a) B. Brunekreef, S. T. Holgate, *Lancet* **2002**, *360*, 1233; b) F. Dominici, R. D. Peng, M. L. Bell, L. Pham, A. McDermott, S. L. Zeger, J. M. Samet, *JAMA, J. Am. Med. Assoc.* **2006**, *295*, 1127; c) R. J. Huang, Y. Zhang, C. Bozzetti, K. F. Ho, J. J. Cao, Y. Han, K. R. Daellenbach, J. G. Slowik, S. M. Platt, F. Canonaco, P. Zotter, R. Wolf, S. M. Pieber, E. A. Brunns, M. Crippa, G. Ciarelli, A. Piazzalunga, M. Schwikowski, G. Abbazade, J. Schnelle-Kreis, R. Zimmermann, Z. An, S. Szidat, U. Baltensperger, I. El Haddad, A. S. Prevot, *Nature* **2014**, *514*, 218; d) A. Peters, H. E. Wichmann, T. Tuch, J. Heinrich, J. Heyder, *Am. J. Respir. Crit. Care Med.* **1997**, *155*, 1376.
- [4] C. A. Pope, D. W. Dockery, *J. Air Waste Manage. Assoc.* **2006**, *56*, 709.
- [5] Y. Li, J. Tao, L. M. Zhang, X. F. Jia, Y. F. Wu, *Int. J. Environ. Res. Public Health* **2016**, *13*, 15.
- [6] a) Y. Chen, S. Zhang, S. Cao, S. Li, F. Chen, S. Yuan, C. Xu, J. Zhou, X. Feng, X. Ma, B. Wang, *Adv. Mater.* **2017**, *29*, 1606221; b) H. M. Xiao, J. Y. Gui, G. J. Chen, C. P. Xiao, *J. Appl. Polym. Sci.* **2015**, *132*, 42807; c) J. Xu, C. Liu, P. C. Hsu, K. Liu, R. Zhang, Y. Liu, Y. Cui, *Nano Lett.* **2016**, *16*, 1270; d) S. Zhang, H. Liu, F. Zuo, X. Yin, J. Yu, B. Ding, *Small* **2017**, *13*, 1603151; e) X. Zhao, Y. Li, T. Hua, P. Jiang, X. Yin, J. Yu, B. Ding, *Small* **2017**, *13*, 1603306; f) S. C. Zhang, H. Liu, X. Yin, Z. L. Li, J. Y. Yu, B. Ding, *Sci. Rep.* **2017**, *7*, 11.
- [7] M. Jerrett, R. T. Burnett, C. A. Pope, K. Ito, G. Thurston, D. Krewski, Y. L. Shi, E. Calle, M. Thun, *N. Engl. J. Med.* **2009**, *360*, 1085.
- [8] M. Zhu, J. Han, F. Wang, W. Shao, R. Xiong, Q. Zhang, H. Pan, Y. Yang, S. K. Samal, F. Zhang, C. Huang, *Macromol. Mater. Eng.* **2017**, *302*, 1600353.
- [9] a) C. He, W. Zhu, B. Chen, L. Xu, T. Jiang, C. B. Han, G. Q. Gu, D. Li, Z. L. Wang, *ACS Appl. Mater. Interfaces* **2017**, *9*, 26126; b) G. Zhu, J. Chen, T. Zhang, Q. Jing, Z. L. Wang, *Nat. Commun.* **2014**, *5*, 3426; c) Z. L. Li, J. L. Shen, I. Abdalla, J. Y. Yu, B. Ding, *Nano Energy* **2017**, *36*, 341; d) J. L. Shen, Z. L. Li, J. Y. Yu, B. Ding, *Nano Energy* **2017**, *40*, 282.
- [10] a) Q. Liang, Q. Zhang, X. Yan, X. Liao, L. Han, F. Yi, M. Ma, Y. Zhang, *Adv. Mater.* **2017**, *29*, 1604961; b) Q. Z. Zhong, J. W. Zhong, B. Hu, Q. Y. Hu, J. Zhou, Z. L. Wang, *Energy Environ. Sci.* **2013**, *6*, 1779.
- [11] a) C. B. Han, C. Zhang, W. Tang, X. H. Li, Z. L. Wang, *Nano Res.* **2014**, *8*, 722; b) C. B. Han, C. Zhang, J. Tian, X. Li, L. Zhang, Z. Li, Z. L. Wang, *Nano Res.* **2014**, *8*, 219; c) S. Wang, Y. Xie, S. Niu, L. Lin, Z. L. Wang, *Adv. Mater.* **2014**, *26*, 2818.
- [12] S. Chen, C. Gao, W. Tang, H. Zhu, Y. Han, Q. Jiang, T. Li, X. Cao, *Z. Wang, Nano Energy* **2015**, *14*, 217.
- [13] G. Q. Gu, C. B. Han, C. X. Lu, C. He, T. Jiang, Z. L. Gao, C. J. Li, Z. L. Wang, *ACS Nano* **2017**, *11*, 6211.
- [14] C. B. Han, T. Jiang, C. Zhang, X. Li, C. Zhang, X. Cao, Z. L. Wang, *ACS Nano* **2015**, *9*, 12552.
- [15] J. Henniker, *Nature* **1962**, *196*, 474.
- [16] a) T. Zhou, L. Zhang, F. Xue, W. Tang, C. Zhang, Z. L. Wang, *Nano Res.* **2016**, *9*, 1442; b) Z. F. Xia, A. Wedel, R. Danz, *IEEE Trans. Dielectr. Electr. Insul.* **2003**, *10*, 102.
- [17] H. Fang, W. Z. Wu, J. H. Song, Z. L. Wang, *J. Phys. Chem. C* **2009**, *113*, 16571.
- [18] a) B. V. Ramarao, C. Tien, S. Mohan, *J. Aerosol Sci.* **1994**, *25*, 295; b) E. A. Ramskill, W. L. Anderson, *J. Colloid Sci.* **1951**, *6*, 416.
- [19] J. L. Allen, X. F. Liu, S. Pelkowski, B. Palmer, K. Conrad, G. Oberdorster, D. Weston, M. Mayer-Proschel, D. A. Cory-Slechta, *Environ. Health Perspect.* **2014**, *122*, 939.
- [20] J. Chen, G. Zhu, W. Yang, Q. Jing, P. Bai, Y. Yang, T. C. Hou, Z. L. Wang, *Adv. Mater.* **2013**, *25*, 6094.
- [21] X. Zhao, S. Wang, X. Yin, J. Yu, B. Ding, *Sci. Rep.* **2016**, *6*, 35472.
- [22] W. Sambaer, M. Zatloukal, D. Kimmer, *Chem. Eng. Sci.* **2011**, *66*, 613.
- [23] D. Hoffmann, I. Hoffmann, K. El-Bayoumy, *Chem. Res. Toxicol.* **2001**, *14*, 767.